The Astrophysical Journal, 628:867–872, 2005 August 1


# OPTICAL AFTERGLOWS OF SHORT GAMMA-RAY BURSTS AND GRB 040924

Y. Z. Fan,[1,2,3] Bing Zhang,[1] Shiho Kobayashi,[4,5] and Peter Mészáros[4,5]
*Received 2004 October 3; accepted 2005 March 15*

## ABSTRACT

Short-duration gamma-ray bursts (GRBs; $\leq$2 s) have remained a mystery due to the lack of afterglow detection until recently. The models to interpret short GRBs invoke distinct progenitor scenarios. Here we present a generic analysis of short GRB afterglows and calculate the optical light curves of short GRBs within the framework of different progenitor models. We show that all these optical afterglows are bright enough to be detected by the Ultraviolet and Optical Telescope (UVOT) on board the *Swift* observatory and that different models could be distinguished with a well-monitored light curve. We also model the afterglow data of the recently discovered short burst GRB 040924. We find that the limited data are consistent with a low medium density environment, which is consistent with the preconcept of the compact star merger progenitor model, although the models with a collapsar progenitor are not ruled out.

*Subject headings:* gamma rays: bursts — ISM: jets and outflows — radiation mechanisms: nonthermal

## 1. INTRODUCTION

In the past several years, great advances have been made in revealing the nature of gamma-ray bursts (GRBs) of relatively long duration, i.e., $T_{90} > 2$ s (e.g., Mészáros [2002] and Zhang & Mészáros [2004] for recent reviews). However, another category of GRBs, i.e., those with short durations (i.e., $T_{90} < 2$ s), which comprise about 1/3 of the total GRB population, have remained as mysterious as long GRBs were before 1997. This has been mainly due to the lack of afterglow detections for short GRBs until very recently.

The leading progenitor model for short GRBs invokes merger of two compact objects (e.g., neutron star–neutron star merger or black hole–neutron star merger; Eichler et al. 1989; Paczyński 1991; Narayan et al. 1992; Mészáros & Rees 1992), which has been found suitable to interpret many short GRB properties (Ruffert et al. 1997; Popham et al. 1999; Perna & Belczynski 2002; Rosswog et al. 2003; Aloy et al. 2004). In this scenario, the burst site is expected to have a large offset from the host galaxy due to asymmetric kicks during the birth of neutron stars (NSs; Bloom et al. 1999; but see Belczynski et al. 2002), so that the number density of the external medium in the GRB environment is low, typically $\sim 10^{-2}$ cm$^{-3}$. Alternatively, with the increasing evidence that long GRB progenitors are collapsars, it has been suggested that short GRBs may also be associated with collapsars, with either a less energetic jet (i.e., short emerging model; Zhang et al. 2003b) or a jet composed of many subjets seen by an off-axis observer looking into one or a few subjet(s) (subjets model; Yamazaki et al. 2004). If this is the case, the environment around the progenitor should be similar to that of long GRBs, which is either a constant-density medium (e.g., Panaitescu & Kumar 2002; Yost et al. 2003) with interstellar medium (ISM) number density $n \sim 1$ cm$^{-3}$ or a prestellar wind (e.g., Chevalier & Li 2000). Other possibilities for the origin of short GRBs have been proposed within the cylindrical jet model (Wang et al. 2005) and the Poynting flux–dominated GRB model (Lyutikov & Blandford 2003).

Within the standard afterglow model and adopting a typical compact star merger environment, the forward shock afterglow emission of short GRBs hase been calculated by Panaitescu et al. (2001), Perna & Belczynski (2002), and Li et al. (2003). Panaitescu et al. (2001) have shown that the afterglows of short GRBs are faint, and they are likely to be most easily detected in the X-ray band. Li et al. (2003) considered possible $e^{\pm}$ pair loading and evaluated its possible observational signature. In this work, we present a generic treatment of short GRB optical afterglows that differs from the previous ones by including both the forward and the reverse shock emission, a crucial ingredient for characterizing the early afterglow light curve and the spectrum. The model is applied to various progenitor models, and sample light curves are calculated, which are compared against the *Swift* UVOT sensitivity (§ 2). Lately, a short, soft burst GRB 040924 was located by the *High Energy Transient Explorer 2* (*HETE-2*), which led to the discovery of its optical afterglow (Fox & Moon 2004). We also apply the model to fit the afterglow data of this burst (§ 3).

## 2. THE AFTERGLOW OF SHORT GAMMA-RAY BURSTS

In the standard afterglow model for a fireball interacting with a constant-density medium (e.g., Sari et al. 1998), for the forward shock (FS) emission, the cooling frequency $\nu_c^f$, the typical synchrotron frequency $\nu_m^f$, and the maximum spectral flux $F_{\nu,\max}^f$ read

$$\nu_c^f = (4.3\times10^{17}\ \mathrm{Hz}) E_{51}^{-1/2}\epsilon_{B,-2}^{-3/2}n_{-2}^{-1}t_d^{-1/2}\left(\frac{2}{1+z}\right), \quad (1)$$

$$\nu_m^f = (3.9\times10^{11}\,\mathrm{Hz}) E_{51}^{1/2}\epsilon_{B,-2}^{1/2}\epsilon_{e,-0.5}^{2}t_d^{-3/2}\left[\frac{13(p-2)}{3(p-1)}\right]^2\left(\frac{2}{1+z}\right), \quad (2)$$

$$F_{\nu,\max}^f = (8.3\mu\ \mathrm{Jy}) E_{51}\epsilon_{B,-2}^{1/2}n_{-2}^{1/2}D_{28.34}^{-2}\left(\frac{1+z}{2}\right), \quad (3)$$

where $E$ is the isotropic energy of the outflow, $\epsilon_B$ and $\epsilon_e$ are the fractions of the shock energy given to the magnetic field and electron at the shock, respectively, $n$ is the number density of

[1] Department of Physics, University of Nevada, Box 454002, 4505 Maryland Parkway, Las Vegas, NV 89154.
[2] Purple Mountain Observatory, Chinese Academy of Sciences, Nanjing 210008, China.
[3] National Astronomical Observatories, Chinese Academy of Sciences, Beijing, 100012, China.
[4] Department of Astronomy and Astrophysics, Pennsylvania State University, 525 Davey Laboratory, University Park, PA 16802.
[5] Department of Physics, Pennsylvania State University, 104 Davey Laboratory, University Park, PA 16802.

the external medium, $p \sim 2.3$ is the power-law distribution index of shocked electrons, $D$ is the luminosity distance, and $z$ is the redshift. Hereafter $t = t_{\rm obs}/(1+z)$ denotes the observer's time corrected for the cosmological time dilation effect and $t_d$ is in units of days. The superscripts $f$ and $r$ represent the forward and reverse shock emission, respectively. Throughout this work, we adopt the convention $Q_x = Q/10^x$ using cgs units. We have normalized the parameters to typical values of short GRBs. The above equations apply to an isotropic fireball or to a jet with opening angle $\theta_0$ when the bulk Lorentz factor $\gamma > 1/(\sqrt{3}\theta_0)$, so that $\gamma \approx 8.2 E_{51}^{1/8} n_{-2}^{-1/8} t_d^{-3/8}$ is satisfied. If sideways expansion is important, for $\gamma \le 1/(\sqrt{3}\theta_0)$, one has $\gamma = (\sqrt{3}\theta_0)^{-1}(t_d/t_{0,d})^{-1/2}$, $F^f_{\nu,\max(J_s)} = F^f_{\nu,\max}(t_d/t_{0,d})^{-1}$, $\nu^f_{c(J_s)} \approx \nu^f_c(t_{0,d})$, and $\nu^f_{m(J_s)} \approx \nu^f_m(t_{0,d})(t_d/t_{0,d})^{-2}$, where $t_{0,d}$ is determined by $1\sqrt{3}\theta_0 = 8.2 E_{51}^{1/8} n_{-2}^{-1/8} t_{0,d}^{-3/8}$ (Rhoads 1999; Sari et al. 1999). If sideways expansion is unimportant, equations (1)–(2) still hold, and equation (3) should be replaced by $F^f_{\nu,\max(J)} \approx F^f_{\nu,\max}(t_d/t_{0,d})^{-3/4}$. Here the subscripts $J$ and $J_s$ represent a jet without and with significant sideways expansion, respectively. During the reverse shock crossing process, the bulk Lorentz factor (LF) of the ejecta is nearly constant if the reverse shock is nonrelativistic (which is the case for short bursts). We have $F^f_{\nu,\max} \propto t^3$, $\nu^f_c \propto t^{-2}$, and $\nu^f_m$ is independent of $t$.

The time when the reverse shock (RS) crosses the shell can be estimated by $t_\times = \max[t_{\rm dec}, T_{90,\rm obs}/(1+z)]$ (Kobayashi et al. 1999). The typical duration of short bursts is $T_{90,\rm obs} \sim 0.2$ s, which is much smaller than the deceleration time $t_{\rm dec}$ for the ISM case. We therefore have a typical thin-shell regime. The RS is only mildly relativistic at the shock crossing time (e.g., Sari & Piran 1999; Kobayashi 2000). The typical deceleration radius is defined as $R_{\rm dec} \approx (5.6\times10^{16}\ {\rm cm}) E_{51}^{1/3} n_{-2}^{-1/3} \eta_{2.5}^{-2/3}$ (Rees & Mészáros 1992), where $\eta \sim 300$ is the initial LF of the outflow. At $R_{\rm dec}$, the LF of the outflow drops to $\gamma_\times = \gamma_{\rm dec} \sim 0.6\eta$, so that $t_{\rm dec} \approx R_{\rm dec}/2\gamma_{\rm dec}^2 c = (30\ {\rm s}) E_{51}^{1/3} n_{-2}^{-1/3} \eta_{2.5}^{-8/3}$.

At $t_\times = t_{\rm dec}$, the LF of the decelerated outflow relative to the initial one is $\gamma_{34,\times} \approx (\eta/\gamma_\times + \gamma_\times/\eta)/2 = 1.13$. The typical frequency of the RS emission can be estimated by

$$\nu^r_m(t_\times) = \mathcal{R}_B \frac{(\gamma_{34,\times}-1)^2}{(\gamma_\times - 1)^2} \nu^f_m(t_\times) \propto n^{1/2}, \quad (4)$$

where $\mathcal{R}_B$ is the ratio of the magnetic field in the RS emission region to that in the FS emission region (Zhang et al. 2003a). Since at least for some bursts (e.g., GRB 990123 and GRB 021211) the RS emission region seems to be more strongly magnetized (e.g., Fan et al. 2002; Zhang et al. 2003a; Kumar & Panaitescu 2003), here we adopt two typical values, i.e., $\mathcal{R}_B = 5$ and 1, in the calculations. There are two possibilities for a magnetized flow (e.g., Fan et al. 2004). The central engine may directly eject magnetized shells. Alternatively, the magnetic fields generated in the internal shock phase may not be dissipated significantly in a short period of time (e.g., Medvedev et al. 2005), and they can get amplified again in the RS region. This second effect, which has been ignored previously, should also play an important role in calculating the afterglow rebrightening effect in refresh-shocks.

Following Kobayashi & Zhang (2003a) and Zhang et al. (2003a), we have

$$\nu^r_c \approx \mathcal{R}_B^{-3} \nu^f_c \propto n^{-1}, \quad (5)$$

$$F^r_{\nu,\max}(t_\times) \approx \eta \mathcal{R}_B F^f_{\nu,\max}(t_\times) \propto n^{1/2}. \quad (6)$$

Generally, the $R$-band flux satisfies $F_{\nu_R}(t_\times) \approx F^r_{\nu,\max}(t_\times)[\nu_R/\nu^r_m(t_\times)]^{-(p-1)/2} \propto n^{\rm p+1/4}$. In the thin-shell case, the $R$-band RS flux is $F^r_{\nu_R} \propto t_{\rm obs}^{2p}$ for $t_{\rm obs} < (1+z)t_\times$ and is $F^r_{\nu_R} \propto t_{\rm obs}^{-2}$ for $t_{\rm obs} > (1+z)t_\times$ (e.g., Sari & Piran 1999; Kobayashi 2000).

If short GRBs are born in a stellar wind (for the collapsar model), for the FS emission, the cooling frequency $\bar\nu^f_c$, the typical synchrotron frequency $\bar\nu^f_m$, and the maximum spectral flux $\bar F^f_{\nu,\max}$ read (Chevalier & Li 2000)

$$\bar\nu^f_c = (2\times10^{13}\ {\rm Hz}) \epsilon_{B,-2}^{-3/2} E_{51}^{1/2} A_*^{-2} \left(\frac{2}{1+z}\right) t_d^{1/2}, \quad (7)$$

$$\bar\nu^f_m = (4.5\times10^{12}\ {\rm Hz}) \epsilon_{e,-0.5}^{2} \epsilon_{B,-2}^{1/2} E_{51}^{1/2} \left(\frac{2}{1+z}\right) t_d^{-3/2}, \quad (8)$$

$$\bar F^f_{\nu,\max} \approx (3.8\ {\rm mJy}) \epsilon_{B,-2}^{1/2} E_{51}^{1/2} A_* D_{28.34}^{-2} \left(\frac{1+z}{2}\right) t_d^{-1/2}, \quad (9)$$

where $A_* = (\dot M/10^{-5}\ M_\odot\ {\rm yr}^{-1})(v_w/10^3\ {\rm km\ s^{-1}})^{-1}$, $\dot M$ is the mass-loss rate of the progenitor, and $v_w$ is the wind velocity. Here the barred parameters represent the wind case.

Equations (7)–(9) apply to an isotropic fireball or to a jet with opening angle $\theta_0$ when the bulk Lorentz factor $\gamma > 1/\sqrt{3}\theta_0$, so that $\gamma \approx 3.3 E_{51}^{1/4} A_*^{-1/4} t_d^{-1/4}$ is satisfied. For $\gamma \le 1/\sqrt{3}\theta_0$, if sideways expansion is significant, the emission properties are similar to the ISM case (Sari et al. 1999; Chevalier & Li 2000). If sideways expansion is unimportant, equations (7)–(8) still hold, and equation (9) should be replaced by $\bar F^f_{\nu,\max(J)} \approx \bar F^f_{\nu,\max}(t_d/\bar t_{0,d})^{-1/2}$, where $\bar t_{0,d}$ is determined by $3.3 E_{51}^{1/4} A_*^{-1/4} \bar t_{0,d}^{-1/4} = 1/\sqrt{3}\theta_0$.

In the wind case, the RS is usually relativistic (e.g., Chevalier & Li 2000). The resulting $t_\times \sim T_{90}$, and the optical emission typically drops as $(t/t_\times)^{-3}$ for $t > t_\times$ (Kobayashi & Zhang 2003b; Kumar & Panaitescu 2000). For short bursts, the duration when the reverse shock emission dominates is too short for any observational interest. In this work, we do not include the RS emission in the wind models. Below we calculate the typical optical-band light curves for short GRBs within different progenitor models.

### 2.1. *Compact Star Merger Model*

The afterglows of short GRBs powered by mergers have been investigated by Panaitescu et al. (2001) numerically. Here we recalculate the optical afterglow light curve by also taking into account the RS emission.

The light curves for this model are plotted as solid lines in Figure 1. At the deceleration time [$\sim 40(1+z)$ s after the burst trigger], the RS emission reaches its peak, and the $R$-band brightness is 20 mag for $\mathcal{R}_B = 5$ (*thin solid line*) and $z = 1$. The *Swift* UVOT has a sensitivity of 24 mag during 1000 s of exposure time. Scaling down with time, the sensitivity should be 19 mag for a 10 s exposure. Unless the event is much closer or $\mathcal{R}_B$ is larger, the RS emission is likely to be below the UVOT sensitivity. The FS emission is quite similar to the numerical calculation of Panaitescu et al. (2001). Because of a lower $n$ and a smaller $E$, the $R$-band afterglow is much dimmer than that of typical long GRBs, but it is still detectable by the UVOT for at least a few hours. In the compact star merger scenario, the collimation of the outflow is quite uncertain. Here we adopt $\theta_0 \sim 0.1$ as suggested in numerical simulations (e.g., Aloy et al. 2004). As shown in Figure 1, the light-curve break occurs too late to be detected with the current telescope sensitivity.

### 2.2. *Short Emerging Model*

In the short emerging model (Zhang et al. 2003b), physical parameters (including the medium density $n$ and the jet opening angle $\theta_0 \simeq 0.1$) are generally similar to those of the familiar

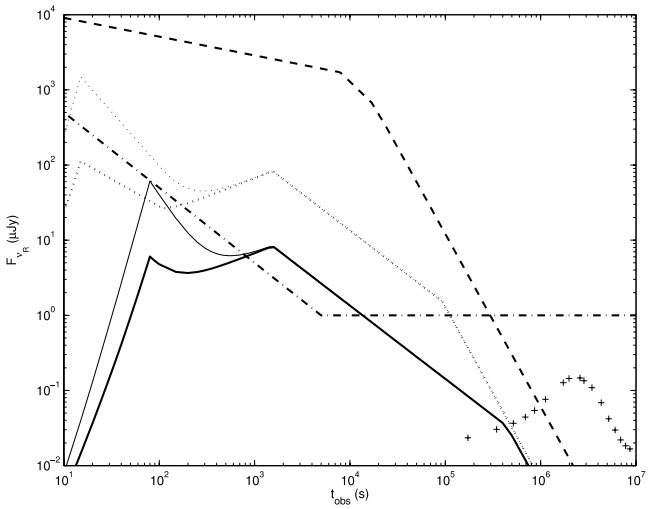


FIG. 1.—Analytical *R*-band light curves of short GRBs in the compact star merger model and the short emerging model. The solid lines, dotted lines, and dashed line represent the compact star merger model in the ISM environment, the short emerging collapsar model in the ISM environment, and the same model in the wind environment, respectively. For the first two models (the ISM models), the reverse shock emission component was calculated for both $\mathcal{R}_B = 5$ (*thin lines*) and $\mathcal{R}_B = 1$ (*thick lines*). The thick dash-dotted line represents the sensitivity of UVOT. For $t_{\rm obs} > 5000$ s, the exposure time of UVOT is assumed to be 1000 s, while for $t_{\rm obs} < 5000$ s, it is assumed to be $t_{\rm obs}/5$. The following parameters are adopted in the calculations: $\eta = 300$, $\epsilon_e = 0.3$, $\epsilon_B = 0.01$, $p = 2.3$, $z = 1$, and $D = 2.2 \times 10^{28}$ cm. In both the compact star merger model and the short emerging ISM model, it is assumed that the outflow is jetlike with an opening angle $\simeq 0.1$ and an isotropic energy $\simeq 10^{51}$ ergs. The ISM number density is taken to be 0.01 and 1 cm$^{-3}$, respectively. For the short merging wind model, the density is taken to be $n = 3 \times 10^{35} R^{-2}$ cm$^{-3}$. For indicative purpose, we also plot a template SN 1998bw–like supernova *R*-band light curve at redshift $z = 1$ (*plus signs*).

long GRBs, except that the isotropic energy is smaller. This model has received support from a recent comparison study of the spectral properties of long and short GRBs (Ghirlanda et al. 2004). The *R*-band light curves of this model are plotted as dotted lines in Figure 1 for the ISM case, where the thin and thick lines are for $\mathcal{R}_B = 5$ and 1, respectively. Compared with the compact star merger model, thanks to a larger $n$ [$F^f_{\nu,\max} \propto n^{1/2}$ and $\nu^f_m \propto n^0$ for $\gamma \geq (\sqrt{3}\theta_0)^{-1}$], the RS peak flux is above the UVOT threshold, if $\mathcal{R}_B$ is somewhat larger than unity. The RS emission peaks earlier (due to a smaller deceleration radius), so that the RS peak may be missed if it is shorter than the slewing time. In any case, the $t^{-2}_{\rm obs}$ decaying component can be detected for $\mathcal{R}_B = 5$ for a $z = 1$ burst. In the wind case, for standard parameters (e.g., $n = 3 \times 10^{35} R^{-2}$ cm$^{-3}$ or $A_* = 1$), the resulting *R*-band light curve is very bright (Fig. 1, *thick dashed line*), thanks to a relative denser medium at $R < 5.5 \times 10^{17}$ cm.

### 2.3. *Subjet Model*

In the subjet model (Yamazaki et al. 2004), GRBs are conjectured as being powered by many intrinsically similar subjets, and the number of the subjets are distributed with angle as a Gaussian function (Zhang & Mészáros 2002), i.e., $n \propto \exp[-(\theta/\sqrt{2}\theta_c)^2]$, with typical Gaussian angle $\theta_c \simeq 0.1$ (Zhang et al. 2004). If an observer is far away from the jet axis and by chance is on the beam of one subjet, one detects a short burst. The global afterglow emission of this model could be then approximated by that of a Gaussian structured jet superimposed on a uniform subjet. Here we consider two emission components, one on-beam uniform less energetic subjet with an opening angle $\theta_{\rm sub} \approx 0.02$ and another stronger and wider Gaussian structured jet with typical Gaussian angle $\theta_c = 0.08$ with the line-of-sight angle $\theta_v \simeq 3\theta_c$ off-axis. Since the Gaussian angular distribution is only of statistical sense in the subjet model (Yamazaki et al. 2004), around the subjet there could be a "void" where the emissivity is below the Gaussian jet model in order to counterbalance the emissivity excess at the subjet. Here we approximate this effect by adopting an annular void region of width $\Delta\theta$ around the subjet axis (i.e., the emissivity is zero in the range from $\theta_{\rm sub}$ to $\theta_{\rm sub} + \Delta\theta$). In view of the uncertainties, we calculate the light curves for $\Delta\theta = 0$, 0.01, 0.02, and 0.03, respectively. Following Yamazaki et al. (2004) we include a maximum Gaussian jet angle $\theta_j = 0.3$ in the calculation.

The afterglow light curves of structured jets have been modeled by many authors (e.g., Wei & Jin 2003; Kumar & Granot 2003; Granot & Kumar 2003; Panaitescu & Kumar 2003; Salmonson 2003; Rossi et al. 2004). Here we take the simple method proposed by Wei & Jin (2003), in which the sideways expansion of the jet is ignored (see Kumar & Granot [2003] for justification) but the "equal arriving surface" effect is taken into account. The jet evolution is quantified by $\gamma = (3\epsilon/n)^{1/2}(m_p c^2)^{-1/2}[ct/(1-\mu+1/16\gamma^2)]^{-3/2}$ for the ISM case and by $\gamma = (\epsilon/3\times10^{35}A_*)^{1/2}(m_p c^2)^{-1/2}[ct/(1-\mu+1/8\gamma^2)]^{-1/2}$ for the wind case.[6] Here $\epsilon = (10^{53}/4\pi)\exp(-\theta^2/2\theta_c^2)$ is the energy per unit solid angle of the structured jet and $\mu = \cos\Theta$, where $\Theta$ is the angle between the moving direction of an emitting unit and the line of sight. The isotropic energy of the on-beam subjet is taken to be $10^{51}$ ergs. The sideways expansion of the on-beam subjet is also ignored. At any emission unit, the standard broken–power-law synchrotron spectrum (e.g., Sari et al. 1998) is adopted with $\delta F^f_{\nu,\max} \approx 3\sqrt{3}\Phi_p(1+z)\delta N_e m_e c^2 \sigma_{\rm T} B/\{32\pi^2 e D^2[\gamma(1-\beta\mu)]^3\}$ (Wijers & Galama 1999), where $\Phi_p$ is a function of $p$ (for $p \simeq 2.3$, $\Phi_p \simeq 0.60$) and $B$ is the magnetic field generated at the shock front. In the ISM case, we take the total number of electrons swept in the solid angle $d\Omega$ as $\delta N_e = d\Omega R^3 n/3$, where $R$ is the radius of the FS front. In the wind case, $\delta N_e = 3.0 \times 10^{35} R\, d\Omega$ is adopted.

The model light curves for the subjet model are plotted separately in Figure 2. The top panel is for the ISM case, and the bottom panel is for the wind case. For a comparison, the light curve of short emerging model is also plotted in each model (*thick solid line*), which is similar to the analytical result presented in Figure 1. For the subjet model, at the early times, the *R*-band emission is dominated by the on-beam subjet. As the subjet is decelerated so that the Lorentz factor is of order $\theta_{\rm sub}$, a very early jet break appears (see Fig. 2 for detail). On the other hand, the energetic Gaussian core component contributes to the emission steadily, becomes progressively important at later times, and dominates the afterglow level after thousands of seconds. Because of the progressively important core contribution, the afterglow decay in the subjet model is much slower than that in the short merging model. Notice that the subjet model could be different from the usual Gaussian jet model in which the angular energy distribution is smooth (e.g., Kumar & Granot 2003; Rossi et al. 2004). The possible existence of the void around the subjet may lead to an afterglow bump (see Fig. 2). In fact, if $\Delta\theta$ is 0.1 or larger, the whole jet can be approximated as two distinct components, i.e., a weak on-beam subjet and an off-beam but more energetic uniform core, since the result is insensitive to the detailed structure in the core. The bump can then be understood in

[6] In the wind case, if we define $X \equiv \epsilon/(3\times10^{35}A_* m_p c^3 t)$, one has $\gamma = \{X(1-\mu) + [X^2(1-\mu)^2 + 4X]^{1/2}\}/2$, and the solutions could be coasted into a simple form.

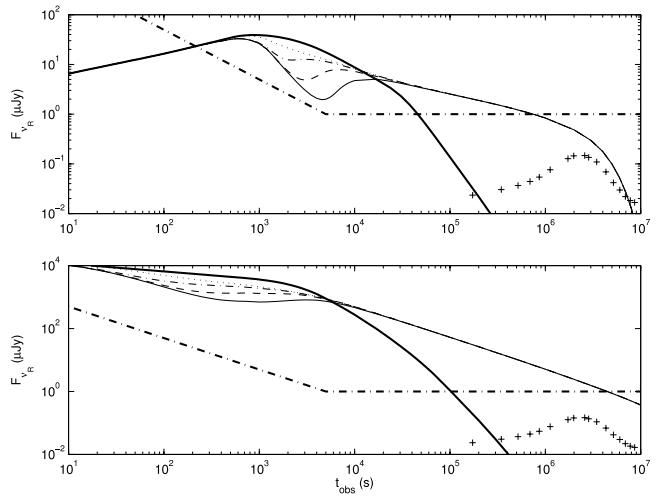


FIG. 2.—*R*-band light curves of short GRBs for the subjet model. The typical light curve for the short emerging model is also plotted for comparison. The top panel is for the ISM case ($n = 1$ cm$^{-3}$), and the bottom one is for the wind case ($n = 3.0\times10^{35}R^{-2}$ cm$^{-3}$). The thin lines are for the subjet model. The dotted, dash-dotted, dashed, and solid lines represent $\Delta\theta = 0$, 0.01, 0.02, and 0.03, respectively. For clarity, only the forward shock emission is taken into account. The following parameters are adopted. For the on-beam subjet, the jet opening angle is $\theta_{\rm sub} = 0.02$, and the isotropic energy is $10^{51}$ ergs. For the Gaussian jet, the typical Gaussian angle is $\theta_c = 0.08$, the maximum angle is 0.3, and angle-dependent energy per solid angle reads $\epsilon = (10^{53}/4\pi)\exp(-\theta^2/2\theta_c^2)$. The line-of-sight angle is $\theta_v = 0.26$ from the jet axis. The thick solid line is for the short emerging model calculated with the same code used to calculate the subjet model. The thick dash-dotted line represents the sensitivity of UVOT. Other parameters such as $\eta$, $\epsilon_e$, $\epsilon_B$, $p$, and $z$ are the same as those adopted to calculate Fig. 1. The supernova bump is also illustrated.

terms of the off-beam orphan afterglow models (e.g., Granot et al. 2002). In our calculations the initial Lorentz factor across the whole jet is assumed to be independent of the angle (Yamazaki et al. 2004).

For both the short emerging model and the subjet model, one may expect a Type Ib or Ic supernova component (usually a red bump) showing up a few weeks after the burst trigger, as has been detected in some long GRBs. For illustrative purpose, we plot in Figures 1 and 2 a template SN 1998bw–like supernova light curve at $z = 1$. The afterglows of short bursts are typically fainter than those of the long ones, so the supernova signature should be easily distinguishable, especially for the short emerging model. For the subjet model, the contamination of the core component may make the identification of the supernova component more difficult. In any case, if a flattening or bump is detected within weeks for a short GRB afterglow, it would argue against the compact star merger model.

## 3. GRB 040924

GRB 040924 triggered *HETE-2* on 2004 September 24 at 11:52:11 UT (Fenimore et al. 2004). The burst lasted $T_{50} \sim 1.2$ s, and the energy fluence was $\mathcal{F}_\gamma \sim 7.7\times10^{-6}$ ergs cm$^{-2}$ (Fenimore et al. 2004; Golenetskii et al. 2004). The ratio of the fluence in the 7–30 keV band and in the 30–400 keV band is about 0.6, so that the burst is classified as an X-ray–rich GRB. The burst redshift was identified as $z = 0.859$ (Wiersema et al. 2004). The prompt localization of GRB 040924 by *HETE-2* allowed follow-up observations of its afterglow at early times (Fox & Moon 2004; Li et al. 2004). Fox (2004) detected an optical transient ~16 minutes after the trigger at the level of $m_R \simeq 18.0$ mag. At the same position, Li et al. (2004) detected an optical transient ~26 and ~63 minutes after the trigger at the level of $m_R \simeq 18.3$ and 19.2 mag, respectively. Later detections in the *K* band and *R* band have been reported by many groups (Terada & Akiyama 2004; Terada et al. 2004; Hu et al. 2004; Fynbo et al. 2004; Khamitov et al. 2004a, 2004b, 2004c). The radio observation provides an upper limit of 0.12 mJy at ~15 hr after the burst (van der Horst 2004). Below we compare the available data with the models, aiming at constraining the burst environment and the possible progenitor.

### 3.1. *ISM Case*

The constraint $F^f_{\nu,\max} \geq 250$ $\mu$Jy results in $f_\gamma \mathcal{F}_{\gamma,-5.1}\epsilon_{B,-2}^{1/2}n_{-2}^{1/2} \geq 1.3$, where $f_\gamma \geq 1$ is the ratio of the afterglow energy to the gamma-ray energy. With $z = 0.859$ and taking $f_\gamma = 2$, we can estimate $E \simeq 3\times10^{52}$ ergs within the standard cosmology. At the time $t_R \leq 945$ s, the typical frequency of the FS emission crosses the observer frequency (*R* band, $\nu_{\rm obs} = 4.6\times10^{14}$ Hz). This results in $0.12\{3(p-1)/[13(p-2)]\}^2(t_R/945\ {\rm s})^{3/2} = E_{52.5}^{1/2}\epsilon_{B,-2}^{1/2}\epsilon_{e,-0.5}^2(1+z)^{1/2}$. We then have the following constraints:

$$\epsilon_e \leq 0.1\left[\frac{3(p-1)}{13(p-2)}\right]\left(\frac{t_R}{945}\right)^{3/4}E_{52.5}^{-1/4}\left(\frac{f_\gamma}{2}\right)^{1/2}\mathcal{F}_{\gamma,-5.1}^{1/2}n_{-2}^{1/4},$$

$$\epsilon_B \geq 4\times10^{-3}\left(\frac{f_\gamma}{2}\right)^{-2}\mathcal{F}_{\gamma,-5.1}^{-2}n_{-2}^{-1}.$$

The observed temporal decay slope is $\alpha_{\rm obs} \simeq -1.07$, which gives $p = 2.42$ in the standard afterglow model. The resulting spectral index $\beta \simeq -0.71$ matches the observation $\beta_{\rm obs} = 0.61 \pm 0.08$ (Silvey et al. 2004). Assuming $t_R \approx 945$ s, $F^f_{\nu,\max} = 250$ $\mu$Jy, and $n = 0.01$ cm$^{-3}$, one gets $\epsilon_e \approx 0.1$ and $\epsilon_B \approx 0.004$. The values of the parameters $\epsilon_e$ and $\epsilon_B$ fall into the regime inferred from afterglow modeling of long bursts (Panaitescu & Kumar 2002; Yost et al. 2003). We note that if we take $n \sim 1$ cm$^{-3}$, $\epsilon_B \sim 10^{-5}$ is obtained. If the shock parameters are more or less universal, our modeling suggests that a low-density ISM model is favored, which is consistent with the preconcept of the merger model. In Figure 3, we use our model light curves to fit the data.

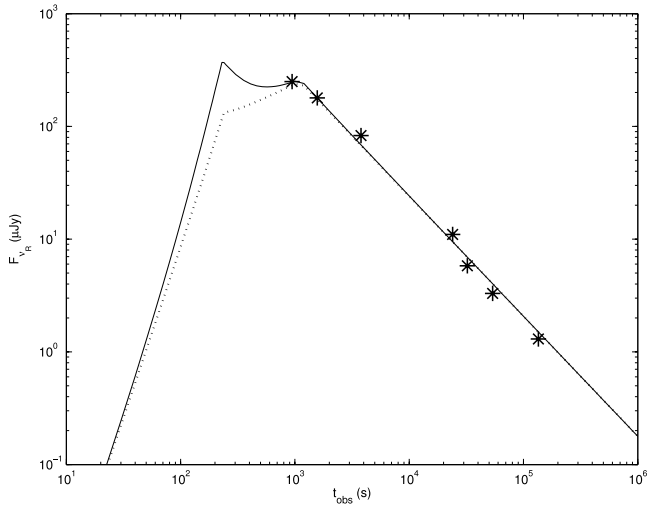


FIG. 3.—Modeling the *R*-band afterglow data of GRB 040924. The identified burst redshift is $z = 0.859$, and the total fluence is $\mathcal{F}_\gamma = 7.7\times10^{-6}$ ergs (Wiersema et al. 2004). This gives $E_\gamma \simeq 1.5\times10^{52}$ ergs, assuming isotropic emission. The data (*asterisks*) are taken from Fox (2004), Li et al. (2004), Hu et al. (2004), and Khamitov et al. (2004a, 2004b, 2004c). The solid and dotted lines are the theoretical afterglow light curves of a slow cooling fireball (or a jet with wide opening angle) expanding into a low-density ISM. The parameters are $E = 3\times10^{52}$ ergs, $f_\gamma = 2$, $\epsilon_e = 0.1$, $\epsilon_B = 0.004$, $n = 0.01$ cm$^{-3}$, and $p = 2.42$. The solid and dotted lines are for $\mathcal{R}_B = 3$ and 1, respectively.

With the parameters derived, $\nu_c^f$ is above the optical energy band throughout the observer time, which is consistent with the observation (Silvey et al. 2004).

### 3.2. *Wind Case*

In the wind case, for $\beta_{\rm obs} \simeq 0.61 \pm 0.08$, and with the temporal index $\alpha_{\rm obs} \simeq -1.07$, $\bar{\nu}_m^f < \nu_{\rm obs} < \bar{\nu}_c^f$ should be satisfied (e.g., Chevalier & Li [2000]; see also the Table 1 of Zhang & Mészáros [2004] for a summary).

At 945 s, the constraints of $\bar{\nu}_c^f > \nu_{\rm obs}$, $\bar{\nu}_m^f \le \nu_{\rm obs}$, and $(\bar{\nu}_m^f/\nu_{\rm obs})^{(p-1)/2}\bar{F}_{\nu,\max} = 250$ $\mu$Jy yield

$$A_* < 0.14\left(f_\gamma/2\right)^{1/4}\epsilon_{B,-2}^{-3/4}, \tag{10}$$

$$\epsilon_{e,-0.5} = 0.09 g^{1/2}\left(f_\gamma/2\right)^{-1/4}\epsilon_{B,-2}^{-1/4}, \tag{11}$$

$$A_* = 5.9\times10^{-4} g^{-(p-1)/2}\epsilon_{B,-2}^{-1/2}\left(f_\gamma/2\right)^{-1/2}. \tag{12}$$

By taking $\epsilon_B \sim 10^{-3}$ and $f_\gamma = 2$, we have $\epsilon_e \sim 0.05 g^{1/2}$ and $A_* \sim 1.8\times10^{-3} g^{-(p-1)} < 0.8$, where we have defined $g = \bar{\nu}_m^f/\nu_{\rm obs}$. Therefore, unless $\epsilon_e$ is much smaller than the typical value of 0.1, we get a very weak stellar wind $A_* \sim 10^{-3}$. A second problem of the wind model comes from the temporal index. For $\beta_{\rm obs} \simeq 0.61$ (Silvey et al. 2004), we have $p \simeq 2.22$, which in turn results in $\alpha \simeq -1.4$. This is significantly steeper than $\alpha_{\rm obs}$. We thus suggest that the wind model is less favored.

In summary, we suggest that the circumburst medium is preferably a constant-density ISM. If we believe that the shock parameters do not vary significantly among bursts, the inferred $n$ is significantly lower than that of the typical ISM, which coincides with the preconcept of the compact objects merger model. No definite jet break is detected, so we do not know the geometrically corrected gamma-ray energy. If GRB 040924 is indeed powered by a merger event, no associated Type Ib or Ic supernova signature (typically a red light-curve bump with flux 1 $\mu$Jy at $z \sim 1$) is expected a few weeks after the burst. The negative detection of the supernova signature at the time when this work is completed (two months after the burst trigger) is also consistent with the compact star merger model.

## 4. SUMMARY AND DISCUSSION

We have modeled the typical optical afterglow light curves for short bursts within the context of the leading progenitor models. Both the forward and reverse shock emission components are considered. With typical parameters, the early afterglows should be detectable by the *Swift* UVOT, and a well-monitored light curve can help to identify the progenitors of short bursts.

The optical afterglow data collected so far for the recent bright short burst GRB 040924 can be modeled well with an isotropic fireball expanding into a low-density medium with $n \sim 10^{-2}$ cm$^{-3}$. The wind model is found to be less favored. The resulting parameters are consistent with the preconcept of the compact star merger model. Other models, such as a collapsar progenitor with low-density environment, however, cannot be ruled out at this stage. In principle, if GRB 040924 came from a collapsar, a light-curve flattening is expected within weeks resulting from either the supernova component or the central core component for the subjet model. The nondetection of such a feature so far presents a further constraint on the collapsar model.

GRB 040924 is a relatively soft event. It may not be a good representative of the traditional short-hard bursts. *Swift* will locate more short-hard bursts, and our analysis could be directly utilized to discuss their nature.

Y. Z. F. thanks D. M. Wei for helpful comments. We also thank the anonymous referee for helpful suggestions. This work is supported by NASA NNG 04GD51G (for B. Z.), Eberly Research Funds of Pennsylvania State, and the Center for Gravitational Wave Physics under grants NSF PHY 01-14375 (for S. K.), NSF AST 00-98416 and NASA NAG5-13286 (for P. M.), and a NASA *Swift* GI (Cycle 1) program (for B. Z., S. K., and P. M.).

## REFERENCES

Aloy, M. A., Janka, H. T., & Müller, E. 2004, A&A, submitted (astro-ph/0408291)
Belczynski, K., Bulik, T., & Kalogera, V. 2002, ApJ, 571, L147
Bloom, J. S., Sigurdsson, S., & Pols, O. R. 1999, MNRAS, 305, 763
Eichler, D., Livio, M., Piran, T., & Schramm, D. N. 1989, Nature, 340, 126
Chevalier, R. A., & Li, Z. Y. 2000, ApJ, 536, 195
Fan, Y. Z., Dai, Z. G., Huang, Y. F., & Lu, T. 2002, Chinese J. Astron. Astrophys., 2, 449
Fan, Y. Z., Wei, D. M., & Wang, C. F. 2004, A&A, 424, 477
Fenimore, E. E., et al. 2004, GCN Circ. 2735 (http://gcn.gsfc.nasa.gov/gcn/gcn3/2735.gcn3)
Fox, D. B. 2004, GCN Circ. 2741 (http://gcn.gsfc.nasa.gov/gcn/gcn3/2741.gcn3)
Fox, D. B., & Moon, D.-S. 2004, GCN Circ. 2734 (http://gcn.gsfc.nasa.gov/gcn/gcn3/2734.gcn3)
Fynbo, J. P. U., Hornstrup, A., Hjorth, J., Jensen, B. L., & Andersen, M. I. 2004, GCN Circ. 2747 (http://gcn.gsfc.nasa.gov/gcn/gcn3/2747.gcn3)
Ghirlanda, G., Ghisellini, G., & Celotti, A. 2004, A&A, 422, L55
Golenetskii, S., Aptekar, R., Mazets, E., Pal'shin, V., Frederiks, D., & Cline, T. 2004, GCN Circ. 2754 (http://gcn.gsfc.nasa.gov/gcn/gcn3/2754.gcn3)
Granot, J., & Kumar, P. 2003, ApJ, 591, 1086
Granot, J., Panaitescu, A., Kumar, P., & Woosley, S. E. 2002, ApJ, 570, L61
Hu, J. H., Lin, H. C., Huang, K. Y., Urata, Y., Ip, W. H., Tamagawa, T., & Fox, D. B. 2004, GCN Circ. 2744 (http://gcn.gsfc.nasa.gov/gcn/gcn3/2744.gcn3)
Khamitov, I., et al. 2004a, GCN Circ. 2740 (http://gcn.gsfc.nasa.gov/gcn/gcn3/2740.gcn3)
———. 2004b, GCN Circ. 2749 (http://gcn.gsfc.nasa.gov/gcn/gcn3/2749.gcn3)
———. 2004c, GCN Circ. 2752 (http://gcn.gsfc.nasa.gov/gcn/gcn3/2752.gcn3)
Kobayashi, S. 2000, ApJ, 545, 807
Kobayashi, S., Piran, T., & Sari, R. 1999, ApJ, 513, 669
Kobayashi, S., & Zhang, B. 2003a, ApJ, 582, L75
———. 2003b, ApJ, 597, 455
Kumar, P., & Granot, J. 2003, ApJ, 591, 1075
Kumar, P., & Panaitescu, A. 2000, ApJ, 541, L51
———. 2003, MNRAS, 346, 905
Li, W., Filippenko, R., Chornock, R., & Jha, S. 2004, GCN Circ. 2748 (http://gcn.gsfc.nasa.gov/gcn/gcn3/2748.gcn3)
Li, Z., Dai, Z. G., & Lu, T. 2003, MNRAS, 345, 1236
Lyutikov, M., & Blandford, R. 2003, preprint (astro-ph/0312347)
Medvedev, M. V., et al. 2005, ApJ, 618, L75
Mészáros, P. 2002, ARA&A, 40, 137
Mészáros, P., & Rees, M. J. 1992, ApJ, 397, 570
Narayan, R., Paczyński, B., & Piran, T. 1992, ApJ, 395, L83
Paczyński, B. 1991, Acta Astron., 41, 257
Panaitescu, A., & Kumar, P. 2002, ApJ, 571, 779
———. 2003, ApJ, 592, 390
Panaitescu, A., Kumar, P., & Narayan, P. 2001, ApJ, 561, L171
Perna, R., & Belczynski, K. 2002, ApJ, 570, 252
Popham, R., Woosley, S. E., & Fryer, C. 1999, ApJ, 518, 356
Rees, M. J., & Mészáros, P. 1992, MNRAS, 258, 41P
Rhoads, J. E. 1999, ApJ, 525, 737
Rossi, E., Lazzati, D., Salmonson, J. D., & Ghisellini, G. 2004, MNRAS, 354, 86
Rosswog, S., Ramirez-Ruiz, E., & Davies, M. B. 2003, MNRAS, 345, 1077
Ruffert, M., et al. 1997, A&A, 319, 122
Salmonson, J. D. 2003, ApJ, 592, 1002
Sari, R., & Piran, T. 1999, ApJ, 517, L109
Sari, R., Piran, T., & Halpern, J. P. 1999, ApJ, 519, L17
Sari, R., Piran, T., & Narayan, R. 1998, ApJ, 497, L17
Silvey, J., et al. 2004, GCN Circ. 2833 (http://gcn.gsfc.nasa.gov/gcn/gcn3/2833.gcn3)
Terada, H., & Akiyama, M. 2004, GCN Circ. 2742 (http://gcn.gsfc.nasa.gov/gcn/gcn3/2742.gcn3)

Terada, H., Akiyama, M., & Kawai, N. 2004, GCN Circ. 2750 (http://gcn.gsfc.nasa.gov/gcn/gcn3/2750.gcn3)
van der Horst, A. J., Rol, E., & Wijers, R. A. M. J. 2004, GCN Circ. 2746 (http://gcn.gsfc.nasa.gov/gcn/gcn3/2746.gcn3)
Wang, X. Y., Cheng, K. S., & Tam, P. H. 2005, ApJ, 621, 894
Wei, D. M., & Jin, Z. P. 2003, A&A, 400, 415
Wiersema, K., Starling, R. L. C., Rol, E., Vreeswijk, P., & Wijers, R. A. M. J. 2004, GCN Circ. 2800 (http://gcn.gsfc.nasa.gov/gcn/gcn3/2800.gcn3)
Wijers, R. A. M. J., & Galama, T. J. 1999, ApJ, 523, 177
Yamazaki, R., Ioka, K., & Nakamura, T. 2004, ApJ, 607, L103
Yost, S., Harrison, F. A., Sari, R., & Frail, D. A. 2003, ApJ, 597, 459
Zhang, B., Dai, X., Lloyd-Ronning, N. M., & Mészáros, P. 2004, ApJ, 601, L119
Zhang, B., Kobayashi, S., & Mészáros, P. 2003a, ApJ, 595, 950
Zhang, B., & Mészáros, P. 2002, ApJ, 571, 876
———. 2004, Int. J. Mod. Phys. A, 19, 2385
Zhang, W., Woosley, S. E., & MacFadyen, A. I. 2003b, ApJ, 586, 356